Leadership in Sustainable Infrastructure

Leadership en Infrastructures Durables

Vancouver, Canada

May 31 – June 3, 2017/ *Mai 31 – Juin 3, 2017*

ANCHORAGE CAPACITY OF TL-5 CONCRETE BRIDGE BARRIER-DECK JUNCTION REINFORCED WITH GFRP BARS AND NEWLY-DEVELOPED 180º HOOKS

Rostami, Michael[1,4], Sennah, Khaled[2], Mostafa, Ahmed[3]

[1] Ph.D. Candidate, Ryerson University, Toronto, Canada

[2] Professor, Ryerson University, Toronto, Canada

[3] Vice President Engineering, TemCorp Industries LTD. Stoney Creek, Ontario, Canada

[4] morteza.fadaee@ryerson.ca

Abstract: The paper presents Glass Fibre Reinforced Polymer (GFRP) bars as an alternative solution to the conventional steel reinforcement in TL-5 concrete bridge barriers due to their corrosion resistance, long-term durability properties and exceptional high tensile strength. To qualify the GFRP-reinforced barrier-deck slab system for use in bridges, the barrier should be designed for vehicle impact to (i) determine the amount of vertical and horizontal reinforcement in the barrier wall and (ii) to determine the bar anchorage details at the barrier-deck slab junction. GFRP bar detailing incorporated the recently-developed high-modulus bars with 180º hook. The goal of this research was to exam the structural qualification of the GFRP bars with 180º hooks for anchorage at the barrier/ deck slab junction. The experimental program consisted of 5 full scale barrier walls with two anchorage profiles to ensure that the resistance of the anchorage at the barrier-deck junction is greater than or equal the factored design load specified in the Canadian Highway Bridge Design Code (CHBDC). Test results justify the barrier design at the barrier-deck junction and the experimental findings are well exceeded the factored applied moments, available in the literature.

1 Background of Research

Ministry of Transportation of Quebec (MTQ) specified TL-5 barrier dimensions and GFRP bar detailing using low-modulus GFRP bars (CSA, 2006). The barrier was developed, tested and approved by MTQ. Pendulum impact test were carried out on this barrier (El-Gamal et al., 2008) considering low-modulus GFRP bars with minimum tensile strengths of 590 MPa and 510 MPa for #5 (15M) and #6 (20M) straight bars, respectively, and minimum tensile strengths of 390 MPa and 300 MPa for #5 and #6 bent bars, respectively (CSA, 2014). Such design is considered outdated given the availability of high-modulus GFRP bars with almost double the tensile strength of the bars currently available. By comparing the GFRP bar details in MTQ PL-3 (currently designated as TL-5) barrier with those with high-modulus, high-tensile-strength GFRP bars in this paper, one may observe the reduction in vertical reinforcement at the front face of the barrier from #6 @ 200 mm to #5 @ 300 mm. Also, the number of horizontal bars reinforcing the barrier wall in the longitudinal direction changes from 14 to 12. Moreover, the vertical bars at the back face of the barrier is reduced from #5 @ 200 mm to #4 (13M) @ 300 mm since these bars are always in compression (Sennah 2016). Most recently, the new TL-5 barrier reinforced with high-modulus and high-tensile-strength GFRP bars was successfully crash tested considering it resting over a cantilever deck slab of 1000 mm width (Sennah, 2016). However, in practice, the connection between the barrier and deck slab may change as a results of changing the GFRP bar anchorage details as the barrier-deck junction or when connection the barrier wall to non-deformable concrete base similar to the solid-slab and voided-slab

bridges. For an anchorage at the barrier-deck slab region to be considered acceptable, significant damage shall not occur in the anchorage or deck during crash testing. If crash testing cannot be conducted to qualify an anchorage design, the anchorage and deck shall be designed to resist the maximum bending, shear, and punching loads that can be transmitted to them by the traffic barrier, except that these loads need not be taken as greater than those resulting from the loads specified in Clause 3.8.8 and applied as specified in CHBDC. CHBDC commentaries (Clause C12.4.3.4.5) suggests the following examples where changes may potentially be acceptable: (i) changes to an anchorage system, where failure of the anchorage is not exhibited during crash testing and the strength of the replacement anchorage is determined to be equivalent to that of the original; and (ii) substituting materials with properties identical or superior to the original material as far as behavior during crash testing is concerned. Since the proposed barrier design reported in this paper was recently crash tested, the proposed changes in this research at the barrier-deck junction can be qualified using static load tests on a constructed barrier segment in the laboratory. CHBDC Clause 12.4.3.5 for barrier anchorage shows that changes may potentially be acceptable if the strength of the replacement anchorage and/or material properties are equivalent or exceed to the original provided the failure of the anchorage is not exhibited during the crash test in the anchorage.

The objective of this practical-design-oriented experimental research program is to (i) determine the ultimate load carrying capacity of the barrier wall-deck slab junction, considering different GFRP bar configurations, when subjected to equivalent transverse vehicle loading, (ii) correlate experimental data with CHBDC design requirements and results from finite-element computer simulation of the barrier-deck system. To perform the above-mentioned static tests on the constructed barriers, CHBDC specifies transverse, longitudinal and vertical forces of 210, 70 and 90 kN, respectively, that can be applied simultaneously over a certain barrier length. CHBDC specifies that transverse load shall be applied over a barrier length of 2400 mm for TL-5 barriers. Since transverse loading creates the critical load carrying capacity at the barrier-deck junction, both the longitudinal and vertical loads were not considered in the design of barrier wall reinforcement and anchorages between the deck slab and the barrier wall. Considering a live load factor of 1.7, the equivalent design impact load on TL-5 barrier over 2.4 m length is 357 kN. CHBDC of 2006 specified factored applied moments for the design of the barrier-deck junction as 83 and 102 kN.m/m at interior and exterior locations of the barrier wall, respectively, shown in Figure 1. However, these values are limited to deck slab cantilever of 1.5 m and do not apply to a rigid deck slab. As a result, finite-element analysis (FEA) was conducted by Azimi et al. (2014b) to examine the effects of barrier length, deck slab thickness and cantilever length on the factored applied moment at the barrier-deck junction of TL-5 barrier. They developed the following equations for the factored design moment at the barrier-deck junction as a function of barrier length, L_b, and deck slab cantilever length, L_c, and thickness, t_s, all in meter units. Based on this analysis, using lateral impact load of 210 kN, distributed over 2400 mm barrier length and located 990 mm over the deck slab surface, the engineer can obtain the applied factored moment at interior and exterior end location of the barrier wall.

[1] $M_{internal}$ = 132 kN.m/m — for fixed base

[2] M_{end} = 148 kN.m/m — for fixed base

[3] $M_{internal} = 100\left(L_b + 2.3t_s\right)^{-1} + 2.83t_s^{0.2}\left(L_b - 1\right)^{0.7} L_c^{-0.8} + 143t_s + 23$ — for cantilever slab (internal part)

[4] $M_{end} = 14t_s^{-1}\left(L_b + 2.3t_s - 2\right)^{-1} + 2.83t_s^{0.2}\left(L_b - 1\right)^{0.7} L_c^{-0.7} + 240t_s + 25$ — for cantilever slab (exterior part)

where t_s is the overhang thickness in meters; L_c is the cantilever length in meters ; L_b is the barrier length in meters, M_{inner} is the moment in the inner portion of barrier in kN.m; M_{end} is the moment in the end portion of barrier in kN.m. The range of parameters used for the parametric study are as follows: 175 mm $\leq t_s \leq$ 350 mm; $0 \leq L_c \leq 2.0$ m and 3.0 m $\leq L_b$.

2 GFRP Bars used in This Study

Glass Fibre Reinforced Polymers (GFRP) bars are non-corrosive materials and considered an excellent alternative to reinforcing steel bars in bridge barriers to overcome steel corrosion-related problems. Grade III-13M (#4) GFRP bars of specified tensile strength of 1135 MPa, modulus of elasticity of 65 GPa and strain at rupture of 1.75%, as listed in the manufacturers catalogue (TEMCORP, 2016), were used in barrier

reinforcement. Also, Grade III-15M (#5) GFRP bars of specified tensile strength of 1620 MPa, modulus of elasticity of 61 GPa and strain at rupture of 2.66% were used in barrier reinforcement. The long-anchored straight portion of Grade III-15M (#5) GFRP bar with 180° hook has specified tensile strength of 1485 MPa, modulus of elasticity of 60 GPa and strain at rupture of 2.40%. However, the bent portion has tensile strength of 905 MPa, modulus of elasticity of 55 GPa and strain at rupture of 1.65%. These 13M and 15M bars have gross cross-sectional area of 132.7 and 240 mm^2, respectively, and nominal cross-sectional areas of 129 and 199 mm^2, respectively. Views of the GFRP bars used in this study are shown in Figure 2. The use of 180° hook and bent GFRP bars are proposed in this research to allow for anchorage in concrete and will be used as deck-barrier conjunction reinforcement.

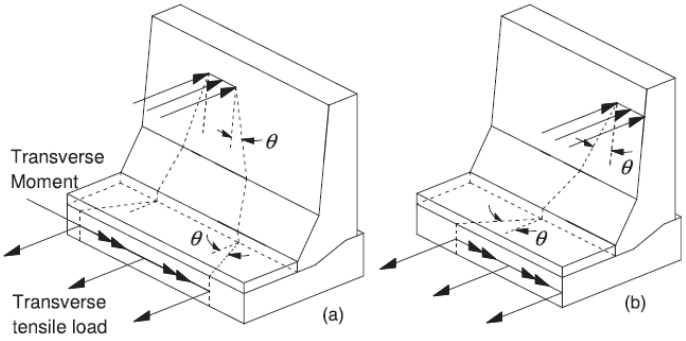

Figure 1: Transverse load dispersion at interior and exterior portions of the barrier wall

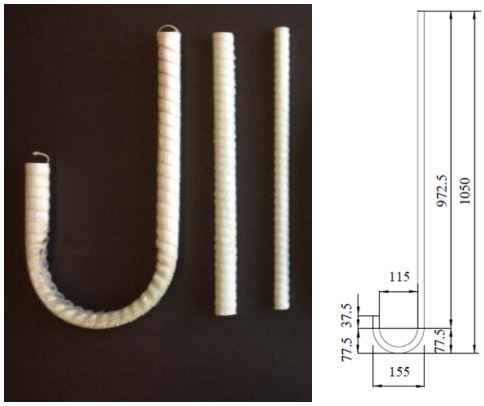

Figure 2: View of GFRP bars used in this study

3 Experimental Program

Five full-scale TL-5 barrier specimens of 900 mm length were erected and tested to-collapse to determine their ultimate load-carrying capacities and failure modes at deck barrier joint. Figure 3 shows a schematic diagram of specimen B-1 that represent the interior segment of the proposed barrier. The barrier is reinforced with M15 GFRP vertical bars at the front face at 300 mm spacing and 13M GFRP vertical bars at the back face of the barrier wall at 300 mm spacing. All vertical GFRP bars are embedded into a 250-mm thick deck slab cantilever with vertical embedment length of 195 mm. The cantilever deck slab was reinforced in the main direction with M20 steel bars at 90 mm spacing. It should be noted the 180º hook was oriented towards the outer face of the barrier wall. Specimen B-2, shown in Fig. 4 was identical to specimen B-1 except in the orientation of the bar hook that was oriented toward the roadway over the bridge deck slab. Specimen B-3 that represents the exterior segment of the proposed barrier. It should be noted that specimen B-3 at exterior location was identical to specimen B-2 at interior location except that the former had the vertical reinforcement at the front face of the barrier doubled. In this case, M15 GFRP vertical bars were used at the front face of the barrier at 150 mm spacing while the vertical reinforcement at the back face of the barrier was kept as M13 at 300 mm spacing. It should be noted that specimens B-2 and B-3 represent barrier construction in case of slab-on-girder bridge system. In case of barrier walls installed on top of solid slab bridges and voided slab bridges, the barrier wall is considered connected to non-deformable thick slab compared to the case of barrier wall installed over 225-mm thick deck slab cantilever in slab-on-girder bridge system. Specimen B-4 shown in Fig. 5 represents this scenario where the barrier wall was fixed to a 500 mm thick slab resting on the laboratory floor to prevent its flexural deformation. The dimensions and GFRP arrangement were the same as those for specimen B-2. The embedment length of the barrier vertical GFRP bars into the thick solid slab base was maintained 195 mm. This specimen represents the case of new construction. Specimen B-5 represents the exterior segment of the proposed barrier rest over thick deck slab. It should be noted that specimen B-5 at exterior location was identical to specimen B-4 at interior location except that the former had the vertical reinforcement at the front face of the barrier doubled. In this case, M15 GFRP vertical bars were used at the front face of the barrier at 150

mm spacing while the vertical reinforcement at the back face of the barrier was kept as M13 at 300 mm spacing. Figure 6 shows a photo of the arrangement of GFRP bars in specimen B-2 before casting concrete.

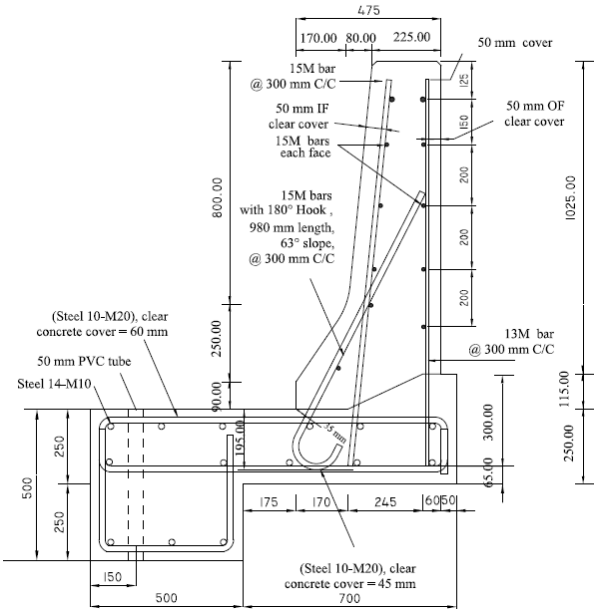

Figure 3: Specimen B-1 for interior portion with hook facing outward at 300 mm spacing

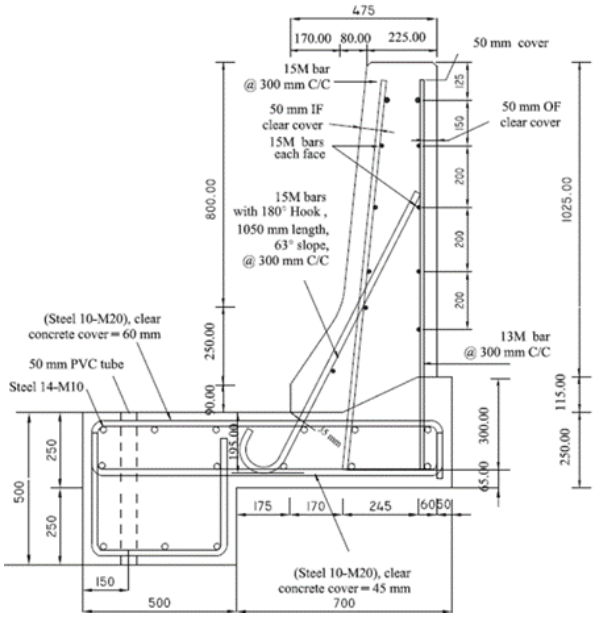

Figure 4: Specimen B-2 for interior portion with 180˚ hook facing inward at 300 mm spacing

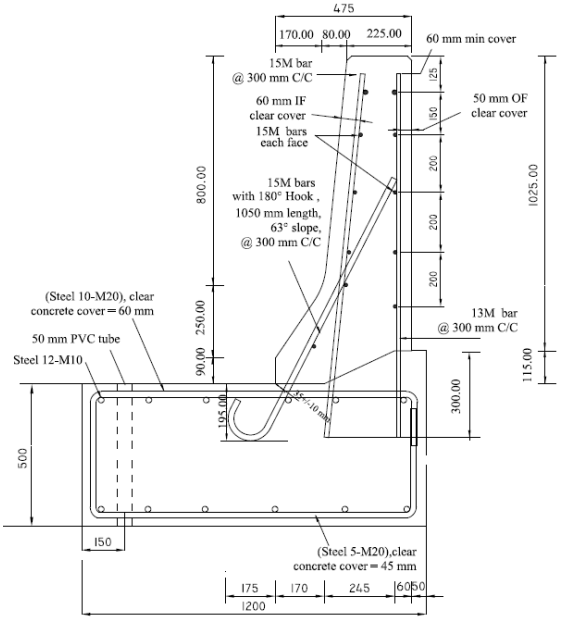

Figure 5: Specimen B-4 for interior portion with 180˚ hook embedded in thick slab at 300 mm spacing

Figure 6: View of internal reinforcement in tested barrier specimen B-2

The characteristic compressive strength of concrete was 50.73 MPa. Figure 9 shows view of the test setup for specimen B-1. Each barrier specimen was supported over the structures laboratory floor, then, tied down to the floor using 50-mm diameter steel threaded rods. Each rod was placed @ 600 mm c-c and tightened by applying a specified torque to control the slab uplift during testing. A hydraulic jack was used to apply horizontal load to the barrier wall. Each specimen was tested under increasing monotonic load up-to-collapse. During the test, jacking load was applied in increments. At each load increment, the load was maintained for a few minutes to observe crack initiation and propagation as well as change in barrier

geometry as depicted from potentiometer (POT) readings. Failure of the model was attained when the readings from sensors were increasing while the model did not take any further increase in load.

Figure 7: Test setup for specimen B-1

Figure 8: Crack pattern on the left side of B-1

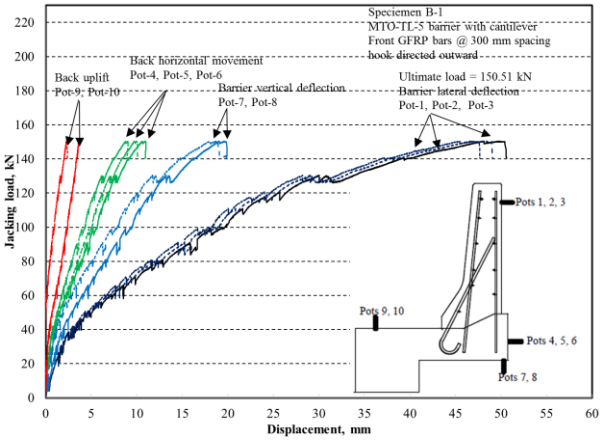

Figure 9: Load-displacement curves for B-1

4 Experimental results

4.1 Specimen B-1

Figure 7 shows the test setup of specimens B-1 before testing. While Fig. 8 shows view of the crack pattern of the tested barrier specimen. In this specimen, the first visible flexural crack was observed at the intersection of the tapered portions of the front side of the barrier wall as well as at the barrier-deck junction and at the deck slab fixed end at 40 kN jacking load. These flexural cracks penetrated further at a higher load, along with other flexural cracks in the deck slab. Although flexural cracks appeared in the barrier wall and the deck slab portion, a sudden diagonal tension crack appeared in the deck slab at a jacking load of 120 kN on the right and left sides of the barrier. These cracks propagated further till the barrier could not take a jacking load beyond 150.5 kN. Given the width of the barrier of 900 mm and the height of the applied load over the top surface of the deck slab of 990 mm, the experimental resisting moment is calculated as 165.56 kN.m/m. This experimental resisting moment at the barrier deck junction is greater than the CHBDC design value of 83 kN.m/m at the barrier-deck slab junction per Table 1 in this report. This leads to a factor of safety of 1.99 in the design of the proposed barrier at interior location as listed in Table 1. Figure 9 depicts the applied load-displacement relationship for specimen B-1. It can be observed that the average deck slab uplift and the horizontal movement at failure were generally equal to 1.95 and 9.71 mm, respectively. These values are considered acceptable and do not significantly affect the structural response of the barrier wall. It can be observed that the maximum lateral deflection of the barrier wall at failure is 46.78 mm, while the barrier vertical deflection is 18.54 mm. Figure 10 depicts the tensile strains in the diagonal GFRP bars at front face of the barrier. Strain gauges were located at 35 mm above the top surface of the deck cantilever as shown in the schematic diagram inserted in the figure. It can be observed that the average strain in the hooked GFRP bars and the adjacent middle GFRP bars at failure were 3892 and 2114 με while the ultimate strain of the GFRP bars per the manufacturer's certification sheet is 26,600 με.

4.2 Specimen B-2

Specimen B-2 is identical to B-1 except that the hook of the diagonal bar at the lower tapered portion at the front face of the barrier wall was oriented to towards the roadway over the deck. Figure 11 shows view of the barrier setup before testing while Fig. 12 shows view of the crack pattern of the tested barrier specimen. In this specimen, the first visible flexural crack was observed in the front side of the barrier wall at barrier-deck junction at 40 kN jacking load. Also, flexural crack appeared at the intersection of the tapered portion of the front side of the barrier wall at a jacking load of 50 kN. Flexural cracks were observed in the deck slab at higher loading. These flexural crack penetrated further into the concrete thickness at a higher load.

However, a sudden diagonal tension crack appeared in the deck slab under the barrier wall at a load of 120 kN. The recorded data in the data acquisition system showed that the barrier could not carry a jacking load beyond 129.92 kN. Given the width of the barrier of 900 mm and the height of the applied load over the top surface of the deck slab of 990 mm, the experimental resisting moment is calculated as 142.91kN.m/m. This experimental resisting moment at the barrier deck junction is greater than the CHBDC design value of 83 kN.m/m at the barrier-deck slab junction per Table 1 in this report. This leads to a factor of safety of 1.72 in the design of the proposed barrier at interior location as listed in Table 1. One may conclude that orienting the 180º hook towards the outer face of the barrier rather than the traffic direction increased the barrier-deck anchorage capacity by 16%. Figure 13 depicts load-displacement relationship for B-2. It can be observed that the average slab uplift and the horizontal movement at failure were 2.89 and 9.76 mm, respectively. It can be observed that the maximum lateral deflection of the barrier wall at failure is 45.51 mm, while the barrier vertical deflection is 16.93 mm.

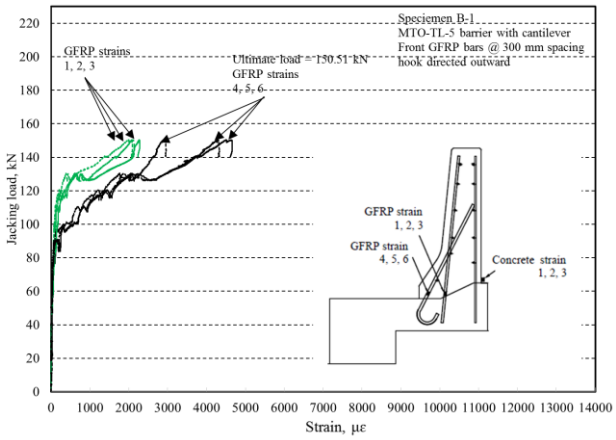

Figure 10: Load-GFRP bar strain curves for B-1

Figure 11: Test setup B-2

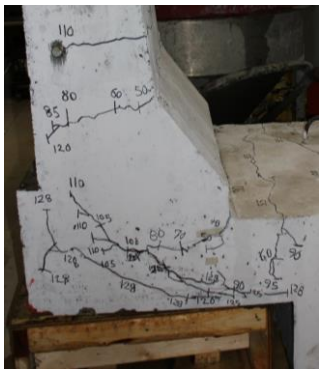

Figure 12: Crack pattern in the left side of B-2

Table 1: Experimental failure loading and comparison with CHBDC-2006 factored design moments at the barrier-deck junction

Barrier specimens / Load description	B-1	B-2	B-3	B-4	B-5
	Interior portion with cantilever slab, 300 mm bar spacing and hook oriented outward	As B-1 but the hook is oriented inward	Exterior portion with cantilever slab, 150 mm bar spacing with hook oriented inward	Interior with non-deformable solid slab, 300 mm bar spacing with hook oriented inward	Exterior non-deformable solid slab, 150 mm spacing with hook oriented inward
Experimental failure load, kN	150.51	129.92	170.33	220.54	328.79
Experimental failure load, kN/m	167.23	144.36	189.26	245.04	365.32
Experimental resisting moment, kN.m/m	165.56	142.91	187.36	242.59	361.67
CHBDC-2006 design moment, kN.m/m	83.00	83.00	102.00	83.00	102.00
Factor of safety (experimental failure moment / CHBDC-2006 design moment)	1.99	1.72	1.84	2.92	3.55
Factor of safety (experimental failure moment/ CHBDC-2006 design moment) with 0.75 durability factor	1.50	1.29	1.38	2.19	2.66

Figure 14 depicts tensile strains in the diagonal GFRP bars at the front face of the barrier. Strain gauges were located at 35 mm above the top surface of the deck cantilever. It can be observed that the average strain in the hooked GFRP bars and the adjacent middle GFRP bars at failure were 4842 and 791 με while the ultimate strain of the GFRP bars per the manufacturer's certification sheet is 26,600 με. The low GFRP

and concrete strain values are attributed to the fact that the failure of the barrier-deck junction is due to diagonal tension in the deck slab cantilever just under the barrier wall.

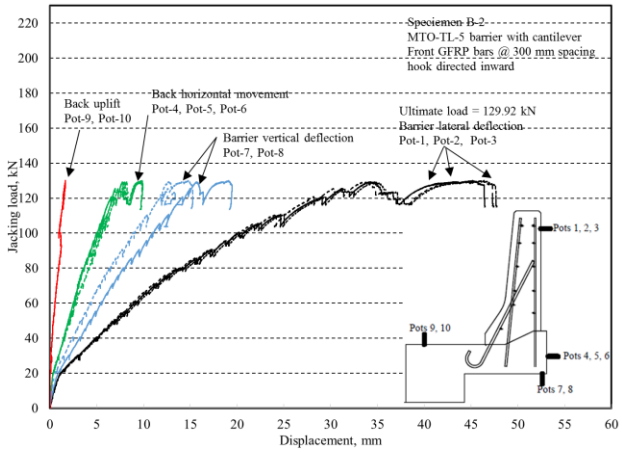

Figure 13: Load-displacement curves for B-2

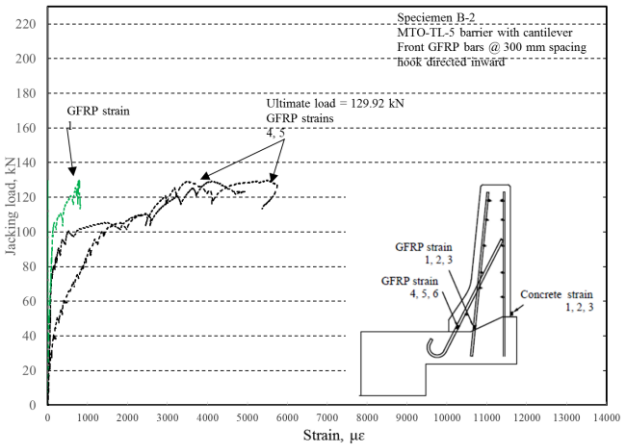

Figure 14: Load-GFRP bar strain curves for B-2

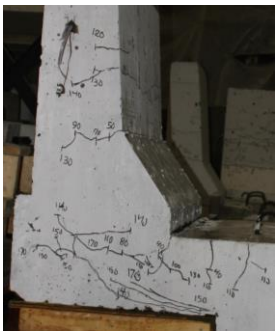

Figure 15: Cracks on left side of B-3

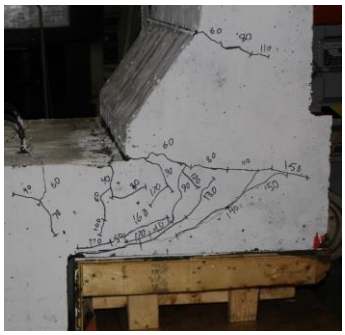

Figure 16: Crack on right side of B-3

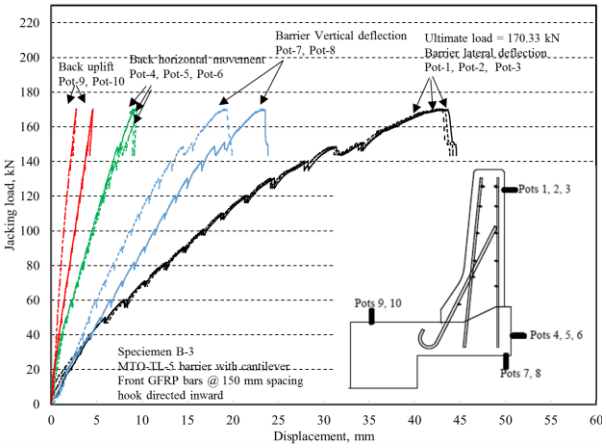

Figure 17: Load-displacement curves for B-3

4.3 Specimen B-3

Specimen B-3 is identical to B-2 except that the vertical bars at the front face of the barrier wall are doubled to represent the exterior location of the barrier wall. Figures 15 and 16 show different views of the crack pattern of the tested specimen. In this specimen, the first visible flexural crack was observed in the front side of the barrier wall at barrier-deck junction at 40 kN jacking load and at the intersection of the tapered portions at 50 kN jacking load. Flexural cracks were observed in the deck slab at jacking load of 50 kN with other flexural cracks appeared at higher loads. These flexural crack penetrated further into the concrete thickness at a higher load. However, a sudden diagonal tension crack appeared in the deck slab under the barrier wall at a load of 140 kN. The recorded data in the data acquisition system showed that the barrier could not carry a jacking load beyond 170.33 kN. Given the width of the barrier of 900 mm and the height of the applied load over the top surface of the deck slab of 990 mm, the experimental resisting moment is calculated as 187.36 kN.m/m. This experimental resisting moment at the barrier deck junction is greater than the CHBDC design value of 102 kN.m/m at the barrier-deck slab junction per Table 1 in this report. This leads to a factor of safety of 1.84 in the design of the proposed barrier at exterior location as listed in Table 1. Figure 17 depicts the applied load-displacement relationship for specimen B-3. It can be observed that the average deck slab uplift and the horizontal movement at failure were 3.66 and 8.98 mm, respectively. These values are considered acceptable and do not significantly affect the structural response

of the barrier wall. It can be observed that the maximum lateral deflection of the barrier wall at failure is 42.5 mm, while the barrier vertical deflection is 21.04 mm. Figure 18 depicts the tensile strains in the diagonal GFRP bars at the front face of the barrier. The strain gauges were located at 35 mm above the top surface of the deck cantilever as shown in the schematic diagram inserted in the figure. It can be observed that the average strain in the hooked GFRP bars and the adjacent middle GFRP bars at failure were 3445 and 686 με while the ultimate strain of the GFRP bars per the manufacturer's certification sheet is 26,600 με.

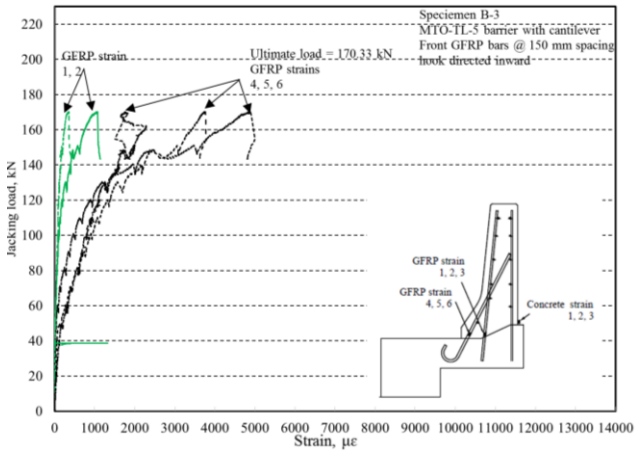

Figure 18: Load-GFRP bar strain curves for B-3

Figure 19: Cracks on left side of B-4

Figure 20: Cracks on right side of B-5

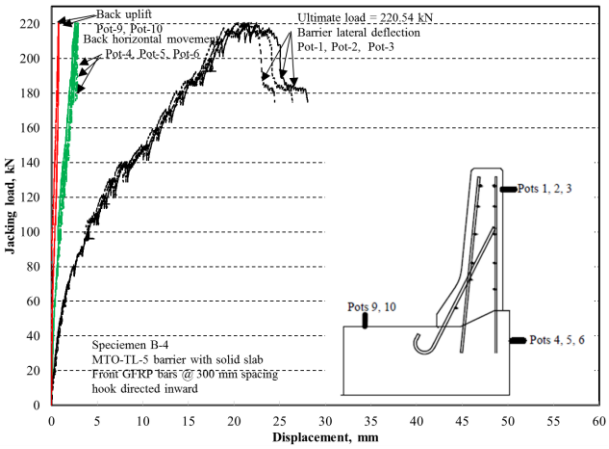

Figure 21: Load-displacement curves for B-4

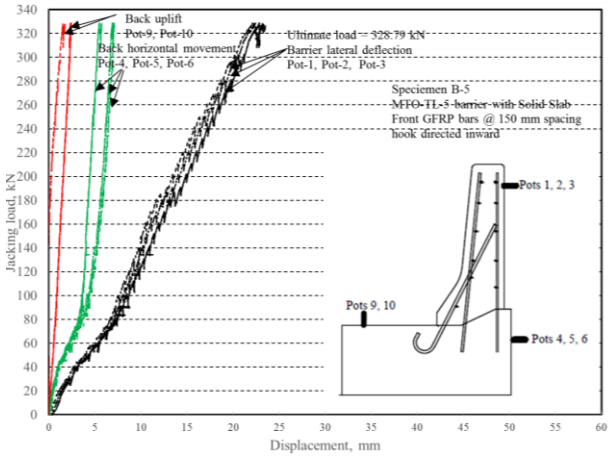

Figure 22: Load-displacement curves for B-5

4.4 Specimen B-4

Specimen B-4 represents a barrier wall connected to non-deformable concrete slab. The amount of vertical reinforcement at the front face represents the case of interior segment of the barrier wall. Figure 19 shows view of the crack pattern after failure. The first flexural crack appeared in the front side of the barrier wall at barrier-deck junction at 30 kN jacking load. Other flexural crack appeared at the intersection of the tapered portions of the front side of the barrier wall at a jacking load of 50 kN. Other extensive flexural cracks appeared in the tapered portion of the barrier at higher loads. Although flexural cracks at the barrier-deck junction penetrated further into the barrier thickness at a higher load giving the signed of flexural failure, sudden concrete shear failure appeared in the top tapered portion of the barrier wall, starting from the applied load location, at a jacking load of 220. 54 kN in each side of the barrier wall. Given the width of the barrier of 900 mm and the height of the applied load over the top surface of the deck slab of 990 mm, the experimental resisting moment is calculated as 242.59 kN.m/m. This experimental resisting moment at the barrier deck junction is greater than the CHBDC design value of 83 kN.m/m at the barrier-deck slab junction

per Table 1 in this report. This leads to a factor of safety of 2.92 in the design of the proposed barrier at interior location when it is rigidly connected to non-deformable concrete deck slab as listed in Table 1. Figure 21 depicts the applied load-displacement relationship for specimen B-4. It can be observed that both the average deck slab uplift and the horizontal movement at failure were 0.80 and 2.78 mm, respectively. These values are considered acceptable and do not significantly affect the structural response of the barrier wall. It can be observed that the maximum lateral deflection of the barrier wall at failure is 21.84 mm which is considered small given the presence of non-deformable deck slab.

4.5 Specimen B-5

Specimen B-5 represents a barrier wall connected to non-deformable concrete slab. The amount of vertical reinforcement at the front face represents the case of exterior segment of the barrier wall. Figure 20 shows different views of the crack pattern of the tested barrier specimen. The first flexural crack appeared in the front side of the barrier wall at barrier-deck junction at 30 kN jacking load. Other flexural crack appeared at the intersection of the tapered portions of the front side of the barrier wall at a jacking load of 60 kN. Other extensive flexural cracks appeared in the tapered portion of the barrier at higher loads. Although flexural cracks at the barrier-deck junction penetrated further into the barrier thickness at a higher load giving the signed of flexural failure, sudden concrete shear failure appeared in the top tapered portion of the barrier wall, starting from the applied load location, at a jacking load of 328.79 kN in each side of the barrier. Given the width of the barrier of 900 mm and the height of the applied load over the top surface of the deck slab of 990 mm, the experimental resisting moment is calculated as 361.67 kN.m/m. This experimental resisting moment at the barrier-deck junction is greater than the CHBDC design value of 83 kN.m/m. This leads to a factor of safety of 3.55 in the design of the proposed barrier at interior location when it is rigidly connected to non-deformable concrete deck slab. Figure 22 depicts the applied load-displacement relationship for specimen B-5. It can be observed that both the average deck slab uplift and the horizontal movement at failure were 1.97 and 6.46 mm, respectively. These values are considered acceptable and do not significantly affect the structural response of the barrier. It can be observed that the maximum lateral deflection of the barrier is 22.5 mm which is considered small given the presence of non-deformable slab.

5 Correlation of Experimental Findings and Results from Finite-Element Modelling

Figure 23 presents correlation between experimental findings and FEA results at the TL-5 barrier's interior location for specimen B-2 with cantilever deck slab and specimen B-4 with thick deck slab.. It can be observed that the FOS for the proposed pre-installed barrier over non-deformable base (specimen B-4) is 1.84 compared to 2.92 obtained based on CHBDC-specified factored applied moment shown in Table 1. As such, it can be concluded that the vertical embedment length of 195 mm for the GFRP bars in the deck slab is adequate to maintain the required barrier-deck anchorage capacity. It can be observed that the FOS for the proposed barrier wall installed over deck slab cantilever increases with increase in deck slab cantilever length, for a given barrier length. Also, it can be observed that the FOS increases with increase of barrier length up to about 6 m, beyond which the increase in FOS is insignificant. It should be noted that for barrier lengths equal of greater than 6 m, the FOS ranges from 1.65 to 2.11 with increase in barrier length up to 12 m, compared to a FOS of 1.72 for specimen B-2 shown in Table 1 based on the available CHBDC design factored moment. Given the barrier length should be long enough to promote two-way action of truck impact load distribution, it is recommended to use the proposed GFRP-reinforced barrier resting over deck slab cantilever, shown in Fig. 3 for barrier length greater than or equal 6 m.

For exterior load location, Figure 24 shows that the FOS for the proposed barrier wall installed over deck slab cantilever increases with increase in deck slab cantilever length, for a given barrier length. Also, it can be observed that the FOS increases with increase of barrier length up to about 6 m, beyond which the increase in FOS is insignificant. It should be noted that for barrier lengths equal of greater than 6 m, the FOS ranges from 1.48 to 2.13 with increase in barrier length up to 12 m, compared to a FOS of 1.84 for specimen B-3 shown in Table 1 based on the available CHBDC design factored moment. Given the barrier length should be long enough to promote two-way action of truck impact load distribution, it is recommended to use the proposed GFRP-reinforced barrier resting over deck slab cantilever for barrier length greater than or equal 6 m. It can be observed that the FOS for the proposed pre-installed barrier over non-deformable base (specimen B-5) is 2.74 compared to 3.55 obtained based on CHBDC-specified factored

applied moment shown in Table 1. Since the scope of this report is to provide experimental findings to qualify the proposed GFRP bar detailing in TL-5 barrier geometries, the experimental factor of safety is considered at least equivalent to 1 to ensure that the experimental capacity is at least equal the factored applied moment at the barrier deck junction specified in CHBDC or obtained by FEA modelling. In case of using experimental findings to qualify the proposed barrier detailing, the resistance factor for design calculation in nonexistence. However, the authors believe that a generic durability factor of 0.75 should apply to the experimental data (CSA, 2014). Figures 23 and 24 present the factors of safety in design of the proposed barrier when a GFRP durability factor of 0.75 is introduced. Although the factor of safety gets smaller with the addition of the durability factor, the conclusions reached earlier are still the same.

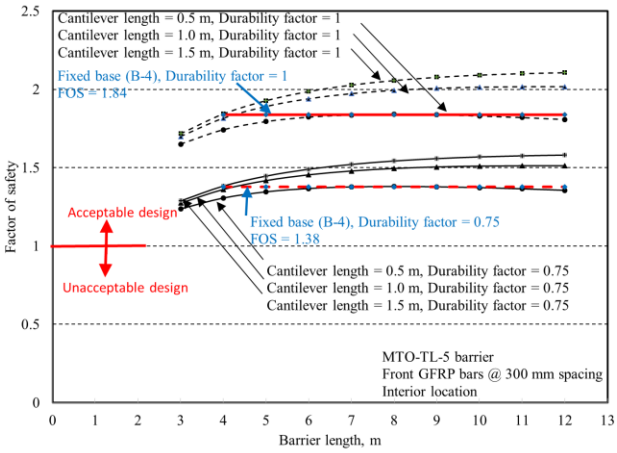

Figure 23: Factors of safety in design at interior location of specimen B-2 with cantilever slab and specimen B-4 for solid slab

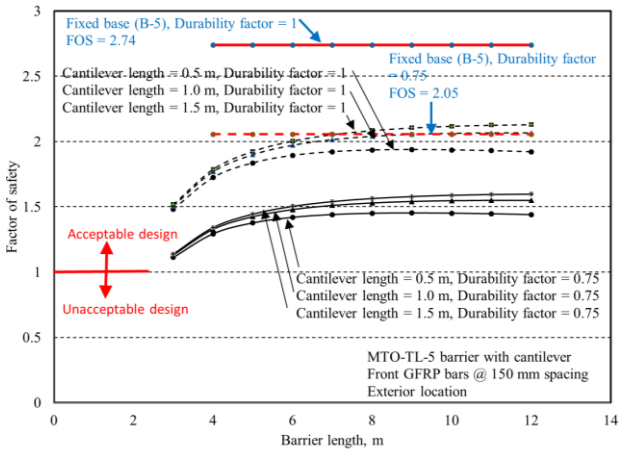

Figure 24: Factors of safety in design at exterior location of specimen B-3 with cantilever slab and specimen B-5 for solid slab

6 Conclusions

Based on the data generated from the experimental program on barrier capacity at the barrier-deck junction, the following recommendation are drawn. The vertical embedment length of 195 mm for the GFRP bars in the deck slab is adequate to maintain the required barrier-deck anchorage capacity. Given the dimensions of the concrete base supporting the barrier wall during tests, the proposed design is acceptable for applications in solid-slab and voided-slab bridge cross-sections with minimum deck slab thickness of 500 mm. Based on the results from the first two specimens, it can be concluded that orienting the 180º hook towards the outer face of the barrier, rather than towards the traffic direction, increased the barrier-deck anchorage capacity by 16%. All barrier specimens B-1 through B-5 showed load carrying capacity at the barrier deck junction greater than the CHBDC applied factored transverse loading.

7 References

Azimi, H., Sennah, K., Tropynina, E., Goremykin, S., Lucic, S., and Lam, M. 2014. Anchorage Capacity of Concrete Bridge Barriers Reinforced with GFRP Bars with Headed Ends. ASCE Journal of Bridge Engineering, 19(9): 1-15.

CSA. 2006. Commentaries on CAN/CSA-S6-06, Canadian Highway Bridge Design Code. Canadian Standard Association, Toronto, Ontario, Canada.

CSA. 2014. Commentaries on CAN/CSA-S6-14, Canadian Highway Bridge Design Code. Canadian Standard Association, Toronto, Ontario, Canada.

El-Gamal, S., Benmokrane, B., and Goulet, S. 2008. Testing of Concrete Bridge Barriers 579 Reinforced with New Glass FRP Bars. Proceedings of the 37th CSCE Annual Conference, 580 Quebec City, Quebec, Canada, CD-Rom: pp.1-10.

Sennah, K. 2016. Vehicle Crash Testing of a PL-3 Concrete Bridge Barrier Reinforced with GFRP TemBars. Technical Report submitted to Temcorp Industries Inc., Stoney Creek, Ontario, pp. 75.

TemCorp Industries Inc., 2016. www.temcorp.ca.